A Global Diagnostic of Interocean Mass Transfers

B. BLANKE AND S. SPEICH

Laboratoire de Physique des Océans, CNRS-IFREMER-UBO, Brest, France

G. MADEC

Laboratoire d'Océanographie Dynamique et de Climatologie, CNRS-IRD-UPMC, Paris, France

K. DÖÖS

Meteorologiska Institutionen, Stockholms Universitet, Stockholm, Sweden

26 April 2000 and 10 October 2000

ABSTRACT

An objective and quantitative estimate of all mean annual interocean mass transfers together with a picture of the associated mean pathways is presented. The global ocean circulation transfers mass, heat, and salinity between the various ocean subbasins on timescales that are likely to interact with the evolution of climate regimes. As an effort to consolidate our knowledge of the present global ocean climatological state, the output of a complex and realistic ocean model is analyzed with newly developed Lagrangian techniques to produce a global circulation scheme that helps and completes our physical understanding of the three-dimensional ocean circulation.

1. Introduction

The ocean exerts a crucial role in the balance of earth's climate and on its evolution on timescales from a few months to several hundred years. However, the detailed structure of currents and water mass displacements are still not well understood. They result from the flow forced by the wind stress at the sea surface and from the thermohaline circulation linked to spatial heterogeneities of the density field. We pose here a general question that arises in physical oceanography: where does the water come from and where does it go? As a response, transports (usually expressed in Sverdrups: Sv $\equiv 10^6$ m^3 s^{-1}) and pathways are often produced by merging distinct sources of data and matching available pieces of knowledge, on a basin (Schmitz and McCartney 1993) or global scale (Macdonald and Wunsch 1996, hereafter MW96; Schmitz 1996, hereafter S96; Sloyan and Rintoul 2000). We show in this study that the output of complex ocean models can be analyzed in a Lagrangian way (Döös 1995; Blanke and Raynaud 1997; Blanke et al. 1999; Speich et al. 2001) so that equivalent schemes might be produced, completing the physical understanding of the three-dimensional ocean circulation.

For the past 15 years, the nature and the very existence of a coherent ocean circulation on the global scale are the topics of permanent debates among physical oceanographers. They distinguish, for instance, a warm route and a cold route for the supply of water into the Atlantic. For the warm route (Gordon 1986), the Pacific and Indian Oceans are linked to the upper Atlantic with an exchange of warm water south of Africa. For the cold route (Rintoul 1991), the dominant contribution of water and heat into the Atlantic is obtained directly at Drake Passage, south of America. The organization of these two routes, with the deep pathway of the southward return flow (along which dense waters progressively spray over the World Ocean bottom before they gradually upwell into the surface layers) defines a circuit called the ''Great Conveyor Belt'' (GCB: Gordon 1986).

Our main results consist in an objective and quantitative estimate of all interocean mass transfers, as well as the picture of the associated mean pathways. The following section describes the Lagrangian methodology, first by introducing the ocean numerical model,

Corresponding author address: Dr. Bruno Blanke, Laboratoire de Physique des Océans, UFR Sciences et Techniques, 6 Avenue Le Gorgeu, BP 809, 29285 Brest Cedex, France.
E-mail: blanke@univ-brest.fr

then by explaining the technique used to quantify the interocean mass transfers. Section 3 details the Lagrangian analysis. A discussion of the results is given in section 4, before conclusions are drawn in section 5. More details about the Lagrangian method are given in the appendix.

2. Methodology

We analyze the velocity field of an ocean general circulation model (OGCM), whose density field is strongly constrained on an observational dataset (Levitus 1982) of temperature and salinity, in order to quantify and picture the global three-dimensional circulation.

a. Ocean model

The OGCM is the Océan Parallélisé (OPA) model (Madec et al. 1998), in its new global configuration. The singularity of the North Pole is removed by introducing an appropriate coordinate transformation (Madec and Imbard 1996) that now includes a double, numerical inland pole. The zonal resolution is 2° within the whole Southern Hemisphere and only slightly distorted in the Northern Hemisphere. The meridional grid interval varies from 0.5° at the equator to a maximum of 1.9° in the Tropics. There are 31 levels in the vertical, with the highest resolution (10 m) in the upper 150 m. The bottom topography and the coastlines are derived from a global atlas (Smith and Sandwell 1997). The model is forced by a daily climatology obtained from the ECMWF 10-yr (1979–88) reanalyses and smoothed by an 11-day running mean. The experiment is designed to recover and study the dynamics associated with the observed global ocean hydrography. Therefore, a restoring term to climatologies (Levitus 1982) is added to the potential temperature and salinity equations, with the coefficient being the inverse of a timescale, varying with depth, and increasing (from zero) with the distances from the coast and the equator (Madec and Imbard 1996). The model vertical physics (Blanke and Delecluse 1993; Beckmann and Döscher 1997) and isopycnal lateral mixing are able to recover the boundary and equatorial currents not well resolved in these climatologies. The OGCM output used for subsequent Lagrangian analyses is averaged over 12 successive monthly periods of the last year of the climatological simulation.

b. Lagrangian tracing

The World Ocean is divided into nine subbasins, limited by model velocity grid points close to convenient geographical limits: both tropics (approximated by latitudes ± 24° on the model mesh) and the Arctic polar circle (approximated by latitude 66°) to distinguish the Arctic, northern, tropical, and southern basins; and the 23°E (south of Africa), 145°E (Tasmania), 65°W (south of America) longitudes and the Indonesian Throughflow (at 125°E) to distinguish the Atlantic, Indian, and Pacific Oceans. As explained with more detail in the appendix for a specific example, systematic Lagrangian experiments equivalent to those introduced in Blanke et al. (1999) are performed for each subbasin, documenting the whole water column in order to compute the mass exchanges between any possible pair of limits, and their associated pathways.

The equations of motion of the OGCM are discretized on a C grid (Arakawa 1972). This differencing turns out ideal for the computation of successive analytical streamlines (Blanke and Raynaud 1997) for given velocity field sampled in time. This mass-preserving trajectory scheme is especially relevant for the tracing of ocean water masses. A water mass on a given geographic section is inseminated with tens or hundreds of thousands of particles (Döös 1995; Blanke and Raynaud 1997), each of which is associated with an infinitesimal fraction of the incoming transport. For selected final destinations (another geographic section, or the fulfillment of a hydrographic criterion), infinitesimal transports may be added, and directional transports can be produced. Off-line diagnostics allow backward computations of trajectories, and the joint use of backward and forward experiments gives access to the error made in computing directional transports, by determining any of them with two independent calculations. Off-line Lagrangian diagnostics also permit looping over a climatological year while calculating trajectories, without the constraint of the true length of the OGCM simulation for setting up the limits of the Lagrangian integration, provided that the simulation is correctly equilibrated (as achieved, in our case, through the use of a climatological forcing and a restoring term added to the temperature and salinity equations). Circulation schemes are obtained by calculating the three-dimensional nondivergent transport field determined by the displacement of the particles and their associated transport and by computing the horizontal streamfunction associated with the vertical integration of this transport field (Blanke et al. 1999).

3. Analysis

Once, all horizontal mass transport streamfunctions, for any possible pair of initial and final sections (of a given subbasin) and associated transmitted transport T_i, an objective circulation scheme is obtained for the global ocean by overlapping the results, with the shallowest exchanges drawn in the foreground and hatching the surface between two contours corresponding to 0.25 T_i and 0.75 T_i so that half of the transmitted mass is accounted by this surface. Additional contours (. . . , $-1.25\ T_i$, $-0.25\ T_i$, . . . , $1.25\ T_i$, $1.75\ T_i$, . . .) are also drawn (if necessary) without hatching to emphasize possible basinwide recirculations associated with interbasin mass transports. Figure 1 presents such a synthetic picture of the mean global ocean circulation, accounting

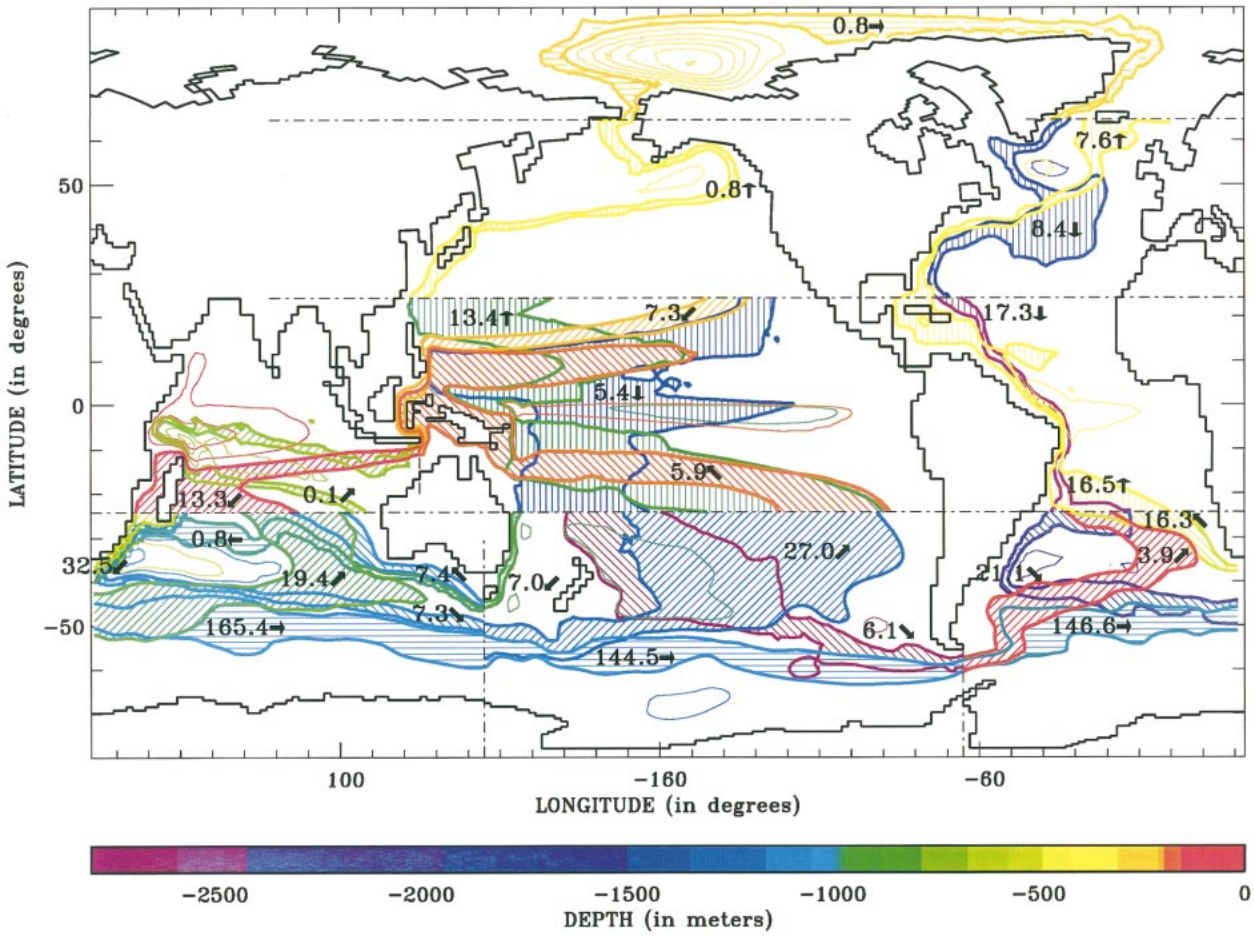

FIG. 1. A global interbasin circulation scheme. Pathways are defined as the median half of each mass transport streamfunction calculated for any pair of given subbasin limits (see text for additional explanations) and are overlapped and colored according to their mean depth, defined as the average of the mean immersions calculated over the initial and final sections (see Table 1). Labels express transports in Sverdrups. The direction of the hatches gives the direction of the flow in the vicinity of the initial and final sections. Arrows document the main orientation of the flow.

for possible seasonal rectification effects as individual trajectories are calculated with a monthly varying velocity field. Table 1 sumps up some useful statistics about mean positions obtained for all mass transfers (on their initial and final sections) from the ensemble of particles used to document them.

The warm colors (light green, yellow, orange, and red) emphasize the so-called upper limb of the GCB. They correspond mostly to a northward transfer of mass throughout the Atlantic Ocean, with water supplied by either the Pacific Ocean through Drake Passage (the ''cold route,'' 3.9 Sv) or the Indian Ocean (the ''warm route''). The Indonesian Throughflow and the southern Atlantic Ocean are both seen to contribute to the warm route, whose intensity (16.2 Sv) is much larger than the cold route. Some Antarctic Circumpolar Current (ACC) water is seen transmitted to the tropical Indian Ocean (19.4 Sv) where it merges with Pacific origin waters. Part of it eventually contributes to the warm route, as proposed by Gordon et al. (1992) from direct measurements and quantified by Speich et al. (2001) with model results.

As the exact origins of the waters entering the Indian Ocean through the Indonesian passages are still a subject of debate (Gordon 1995; Lukas et al. 1996; Shriver and Hurlburt 1997), the contributions found from the northern (7.3 Sv) and southern (5.9 Sv) Pacific Ocean define a valuable result. Southern origin waters exhibit more complex and longer pathways in the tropical Pacific, with some circulation in both the North and South Equatorial Currents; they undergo more intense conversions induced by air–sea interactions (warming and freshening) and are associated mostly with the upper layers of the Indonesian Throughflow (Table 1). Northern origin waters follow a more direct way toward the throughflow, probably after subduction in the North Pacific, having first crossed the whole tropical Pacific and circulated in the north subtropical and, possibly, subpolar gyres.

The cold colors (purple, blue, and dark green) used in Fig. 1 refer to the deep limb of the same GCB. Again,

TABLE 1. Statistics for all interbasin mass transfers and intrabasin recirculations. Transport and mean positions (with associated standard deviations) for (a) all diagnosed interbasin mass transfers and (b) intrabasin recirculations. Mean positions and standard deviations are obtained from the ensemble of particles used to describe the transfers. (Th-Flow ≡ throughflow.)

(a) Interbasin mass transfers

Initial section	Final section	Transport (Sv)	*x* initial (deg)	*x* final (deg)	*y* initial (deg)	*y* final (deg)	*z* initial (m)	*z* final (m)
Africa 23°E	Tasmania 145°E	165.4	23	145	−48 ± 4	−56 ± 5	1016 ± 780	1014 ± 855
America 65°W	Africa 23°E	146.6	−65	23	−59 ± 2	−49 ± 4	1094 ± 869	871 ± 699
Tasmania 145°E	America 65°W	144.5	145	−65	−56 ± 4	−59 ± 2	1033 ± 782	1009 ± 825
Indian 24°S	Africa 23°E	32.5	42 ± 7	23	−24	−38 ± 1	598 ± 484	561 ± 513
Tasmania 145°E	Pacific 24°S	27.0	145	−131 ± 38	−53 ± 5	−24	984 ± 1233	1517 ± 1732
Atlantic 24°S	Africa 23°E	21.1	−30 ± 14	23	−24	−47 ± 4	2348 ± 1077	2309 ± 769
Africa 23°E	Indian 24°S	19.4	23	83 ± 17	−47 ± 5	−24	523 ± 972	1090 ± 1410
Atlantic 24°N	Atlantic 24°S	17.3	−66 ± 11	−28 ± 14	24	−24	2331 ± 701	2700 ± 633
Atlantic 24°S	Atlantic 24°N	16.5	−14 ± 17	−76 ± 18	−24	24	424 ± 381	349 ± 497
Africa 23°E	Atlantic 24°S	16.3	23	−13 ± 17	−37 ± 2	−24	614 ± 812	514 ± 487
Pacific 24°S	Pacific 24°N	13.4	−118 ± 33	148 ± 37	−24	24	1118 ± 1590	795 ± 1469
Th-flow 125°E	Indian 24°S	13.3	125	60 ± 29	−10 ± 1	−24	105 ± 109	98 ± 202
Atlantic 66°N	Atlantic 24°N	8.4	−29 ± 12	−68 ± 11	66	24	575 ± 444	2530 ± 791
Atlantic 24°N	Atlantic 66°N	7.6	−79 ± 10	−15 ± 13	24	66	504 ± 236	316 ± 168
Tasmania 145°E	Indian 24°S	7.4	145	91 ± 13	−45 ± 1	−24	974 ± 404	1034 ± 579
Indian 24°S	Tasmania 145°E	7.3	52 ± 11	145	−24	−52 ± 5	880 ± 1073	1265 ± 1126
Pacific 24°N	Th-flow 125°E	7.3	−138 ± 11	125	24	−10 ± 1	260 ± 410	143 ± 108
Pacific 24°S	Tasmania 145°E	7.0	157 ± 6	145	−24	−45 ± 1	943 ± 531	946 ± 356
Pacific 24°S	America 65°W	6.1	−168 ± 23	−65	−24	−58 ± 2	2776 ± 829	2574 ± 765
Pacific 24°S	Th-flow 125°E	5.9	−106 ± 23	125	−24	−11 ± 1	315 ± 523	49 ± 36
Pacific 24°N	Pacific 24°S	5.4	−136 ± 26	−175 ± 35	24	−24	1792 ± 1603	1087 ± 1187
America 65°W	Atlantic 24°S	3.9	−65	−26 ± 8	−59 ± 2	−24	28 ± 46	214 ± 143
Tasmania 145°E	Africa 23°E	0.8	145	23	−50 ± 8	−44 ± 12	809 ± 394	1150 ± 561
Pacific 66°N	Atlantic 66°N	0.8	−170 ± 1	−30 ± 13	66	66	16 ± 8	417 ± 467
Pacific 24°N	Pacific 66°N	0.8	125 ± 6	−170 ± 1	24	66	821 ± 733	16 ± 8
Indian 24°S	Th-flow 125°E	0.1	107 ± 4	125	−24	−10 ± 0	799 ± 296	742 ± 63

(b) Intrabasin recirculations

Initial section	Way	Transport (Sv)	*x* initial (deg)	*x* final (deg)	*y* initial (deg)	*y* final (deg)	*z* initial (m)	*z* final (m)
Pacifc 24°N	North	73.0	143 ± 32	−178 ± 37	24	24	1031 ± 1349	1064 ± 1325
Pacific 24°N	South	60.3	174 ± 34	141 ± 30	24	24	1106 ± 1332	1074 ± 1302
Indian 24°S	North	55.6	81 ± 21	55 ± 20	−24	−24	1223 ± 1361	1076 ± 1111
Africa 23°E	West	49.6	23	23	−52 ± 13	−49 ± 7	1507 ± 1368	1309 ± 1205
Pacific 24°S	North	46.3	−150 ± 41	−166 ± 45	−24	−24	1456 ± 1447	1259 ± 1213
Pacific 24°S	South	38.6	−160 ± 48	−145 ± 43	−24	−24	1049 ± 1183	1102 ± 1189
Atlantic 24°N	North	37.7	−68 ± 21	−54 ± 20	24	24	973 ± 1377	1309 ± 1265
Africa 23°E	East	32.5	23	23	−54 ± 6	−59 ± 11	1911 ± 1204	2004 ± 1456
Indian 24°S	South	29.0	72 ± 25	76 ± 24	−24	−24	1213 ± 1413	1368 ± 1450
Atlantic 24°N	South	28.6	−50 ± 21	−66 ± 20	24	24	1031 ± 1320	1173 ± 1437
Atlantic 24°S	North	16.4	−18 ± 17	−19 ± 20	−24	−24	1399 ± 1445	1384 ± 1380
Atlantic 66°N	North	13.8	−15 ± 13	−26 ± 13	66	66	326 ± 307	557 ± 438
Atlantic 24°S	South	12.6	−13 ± 19	−17 ± 16	−24	−24	1551 ± 1350	1637 ± 1496
Atlantic 66°N	South	6.2	−23 ± 14	−16 ± 13	66	66	524 ± 428	350 ± 432
Tasmania 145°E	East	2.9	145	145	−51 ± 7	−50 ± 8	1263 ± 921	1071 ± 743
Tasmania 145°E	West	1.7	145	145	−51 ± 9	−51 ± 7	1072 ± 834	1231 ± 791
Th-flow 125°E	East	0.6	125	125	−10 ± 2	−10 ± 2	672 ± 374	712 ± 414
Th-flow 125°E	West	0.5	125	125	−10 ± 1	−10 ± 2	672 ± 400	680 ± 382

the Atlantic Ocean is the main place where these transfers occur, with the formation of dense waters in the Arctic Ocean (8.4 Sv). The choice of the Arctic Circle as a northern limit of the North Atlantic separates the deep water formed in the arctic domain (Greenland and Norway Seas) from the water entrained immediately downstream the main arctic straits (Denmark Strait and Iceland–Scotland passage). The water formed in the Labrador Sea is also excluded from the 7.6/8.4 Sv evaluation of the overturning in the North Atlantic, and must appear at the same level as Mediterranean Water or subducted subtropical water, that is, as water converted in the North Atlantic basin (between 24°N and the Arctic Circle). The full amplitude of the North Atlantic Deep Water overturning is, in fact, to be read in the tropical Atlantic (16.5/17.3 Sv). The deep circulation in the

North Atlantic consists of a deep western boundary current and a southward flow east of the Mid-Atlantic Ridge. This last path (accounting for two-fifths of the transport) confirms and quantifies some hypotheses already formulated about the presence of a southward flow of Labrador Sea Water in the eastern Atlantic (Paillet et al. 1998).

The tropical Pacific Ocean is fed from the ACC (27.0 Sv) at a deeper mean immersion than the Indian Ocean. Although this depth (at 145°E) seems linked to intermediate layers, one must not forget that the 27 Sv include the whole flow transmitted from the southern Indian Ocean to the tropical Pacific. This value therefore also accounts for surface and subsurface as well as for deep waters. As diagnosed, for instance by Reid (1997) or Tsimplis et al. (1998), there is indeed a net inflow of Antarctic Bottom Water and Lower Circumpolar Water to the Pacific (from the south) as well as an inflow of Antarctic Intermediate Water. These inflows are balanced in a model by a net outflow of Pacific Deep Water (6.1 Sv, lying between these inflows), a southwestward supply of intermediate water along the southeastern Australian coast (7.0 Sv) that clarifies the origin of an additional component found for the warm route of the GCB (Speich et al. 2001) by linking it to the South Pacific subtropical gyre and the Indonesian Throughflow (13.3 Sv). Part of the Pacific northward flow originating in the Indian Ocean eventually crosses both tropics (13.4 Sv) and reaches the North Pacific. The uppermost fraction contributes to the northern branch of the Indonesian Throughflow alimentation, while the deeper layers flow back to the South Pacific (5.4 Sv), as a combination of Pacific Deep Water and intermediate water.

Large-scale recirculations are also found through the Lagrangian analysis and correspond mostly to the basin-scale subtropical gyres directly forced by the wind. The subpolar gyre in the northern Atlantic Ocean as well as the intense cyclonic recirculation of the Weddell Sea in the southern Atlantic, also with a signature in the Indian Ocean, appear too. These recirculations are presented in Fig. 2 with a contour interval adapted to each case. The analysis only evidences recirculation loops that intersect at least one of the geometrical limits chosen to divide the global ocean. Other recirculations do exist but are enclosed in a given subbasin (e.g., the Ross Sea gyre in the southern Pacific). Local dominant upwelling or downwelling phenomena can be detected by comparing the mean depth between the beginning and the end of each transfer (Table 1). The tropical Pacific and Indian Oceans as well as the ACC area display obvious dispositions for upwelling. Downwelling areas correspond to the formation and spreading of dense waters in the Atlantic, and to the external (off tropical) fractions of all subtropical gyres where seasonal subduction phenomena can inject surface water into the ocean interior.

4. Discussion

The joint use of backward and forward Lagrangian calculations gives access to a measurement of the error made in computing directional transports, as any transport (from section A to section B) can be calculated in two independent ways: inseminating A and summing the transports of the particles that reach B, or inseminating B and summing the transports of the particles that originate in A. The size of the resulting error is roughly of the order of the infinitesimal transport given to each individual particle, here 10^{-2} Sv. It allows us to define all our Lagrangian transports with an accuracy better than 0.1 Sv. The Lagrangian experiments are carried out separately for each ocean basin. This approach explains the discontinuities observed on the mean depths of the transfers or on the contours drawn near the junction between two basins. The transports, however, coincide (to within about 0.1 Sv) on each section, as the transmitted and net flows must be the same when considered in either of two neighboring basins (see Fig. 1).

Because the ocean eddies are not sampled in this model, due to a too low lateral resolution, the results can only address the large-scale patterns of the global circulation. Their direct effect on the interbasin exchanges is not, however, neglected since their signature is present in the climatological temperature and salinity fields used to constrain the model mass field in the ocean interior. Used in conjunction with appropriate lateral and vertical physics, this restoring term allows the calculation of a realistic climatological year over the whole domain (Blanke et al. 1999), despite the other caveats the model may include, as a coarse vertical resolution within the ocean bottom layers or the use of a poorly energetic, low frequency, climatological atmospheric forcing. The main purpose of our Lagrangian calculations is not, indeed, the computation of complex individual trajectories that should fit the movement of genuine water particles, but the diagnostic of robust large-scale streamlines, fully compatible with the description of the mean seasonal global ocean circulation.

A direct, systematic, comparison of global water mass transports with already published material is somewhat uneasy, as the mass fluxes we diagnose are only dependent on a geographical choice of initial and final sections. Direct estimates are usually associated with a careful hydrographic analysis of Eulerian flows, splitting the transport into distinct water masses (as surface, deep, and bottom waters), and establishing correspondences with different hydrographic sections. A few key points of the GCB may, however, be compared. The total northward transmitted flow in the tropical Atlantic (16.5 Sv) is, for instance, coherent with the northward flow proposed by S96 (18 Sv). Our total ACC transport at Drake Passage (150.5 Sv) fits the estimate by MW96 [142 Sv, with roughly a 10 Sv uncertainty, constrained with Whitworth et al. (1982) current-meter measure-

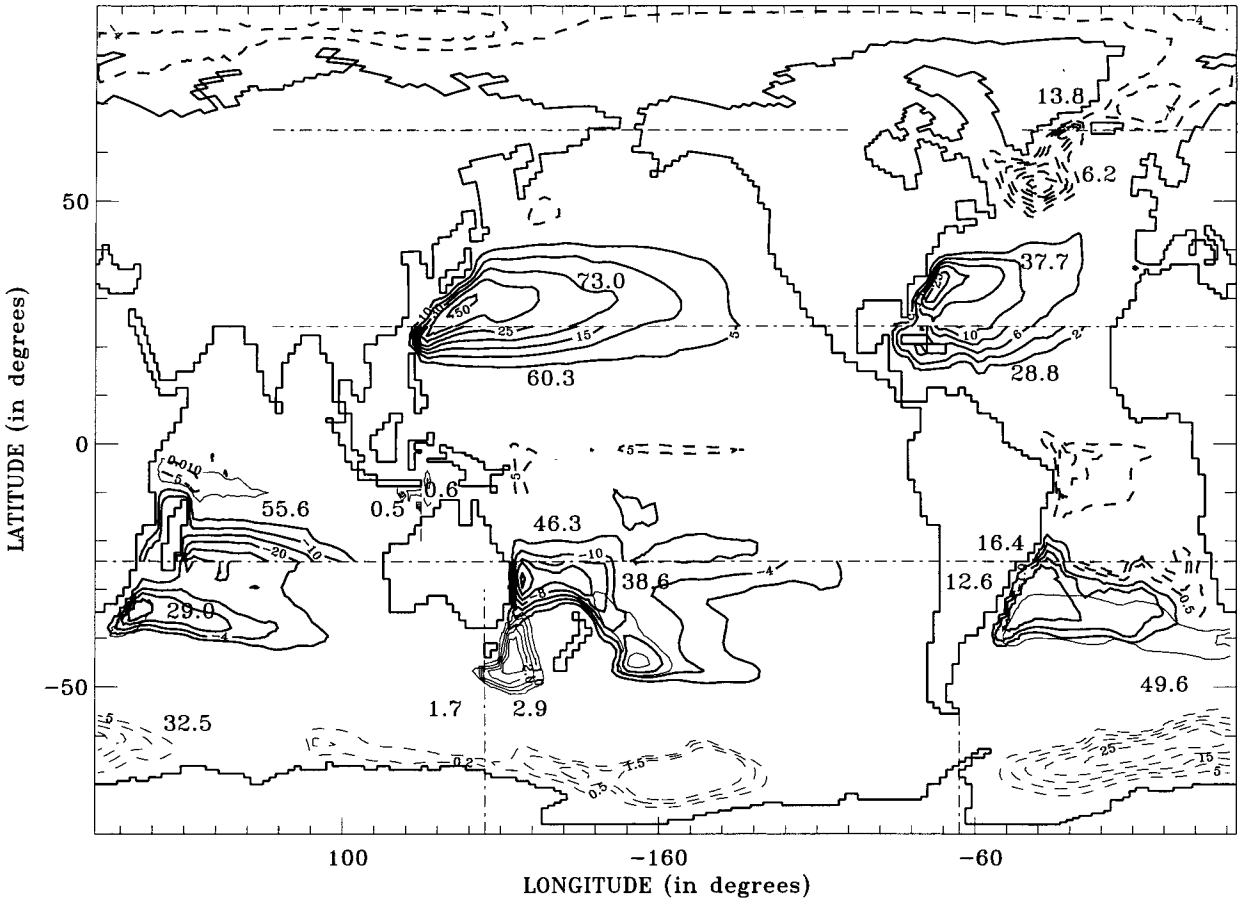

FIG. 2. Intrabasin recirculations. Pathways are pictured with a few contours of the mass transport streamfunctions calculated for each possible recirculation (over a given initial section). The contour interval is adapted for each recirculation and the zero is chosen on a nearby coastline intercepted by the initial section. Meridional and zonal recirculations are displayed with thick and thin contours, respectively. Dashed contours denote a cyclonic circulation. The pictured maximum is often smaller than the exact value (i.e., the label expressed in sverdrups) diagnosed from the Lagrangian experiments since the journey from and back to the initial section may occur at equivalent longitudes (or latitudes) but distinct depths and, thus, compensate each other when pictured with a two-dimensional streamfunction (Blanke et al. 1999), or may be associated to partially cyclonic and anticyclonic motions (e.g., south of Africa).

ments]. Our Pacific–Indian flow through the Indonesian passages (13.8 Sv) fits the recent measurements of Gordon et al. (1999) for a null ENSO index (12 Sv). The intensities of our subtropical cells prove comparable to those of MW96 when calculated at equivalent latitudes (as both tropics in the Pacific). Finally, the transport of Indian Ocean water to the tropical Pacific (27 Sv) matches the value proposed by S96 for the transfer of bottom and upper ocean ACC water toward the same area. As our diagnostics truly distinguish transmitted (Fig. 1) and recirculating (Fig. 2) flows, the proposed pathways offer an interesting complement to global schemes viewed as in MW96, by highlighting major connections achieved within each basin, isolating them from the intense flows associated with the subtropical or polar gyres.

5. Conclusions

A global picture of interocean mass transfers is obtained by means of an OGCM constrained on observed climatologies (Levitus 1982) for temperature and salinity, and acting as a dynamical interpolator. This constraint forces the model to diagnose a large-scale circulation (mostly geostrophic in the ocean interior) in agreement with the flow that could have been calculated directly from the climatologies. It leads to Eulerian transport estimates, diagnosed at selected latitudes and longitudes, in fair agreement with values inferred from direct measurements and forms a solid basis for subsequent Lagrangian diagnostics. Besides different known connections, our results add new possible links between subbasins and evaluate precisely and objectively their intensity and geometry, distinguishing intrabasin recirculations (as subtropical gyres) and interbasin connections. The approach adopted in this study does not distinguish layered flows, except if they correspond to distinct interbasin transfers, but is confined to a depth-integrated vision of the mass flow. More selective criteria based on hydrography will be developed in the future for the definition of the initial positions of

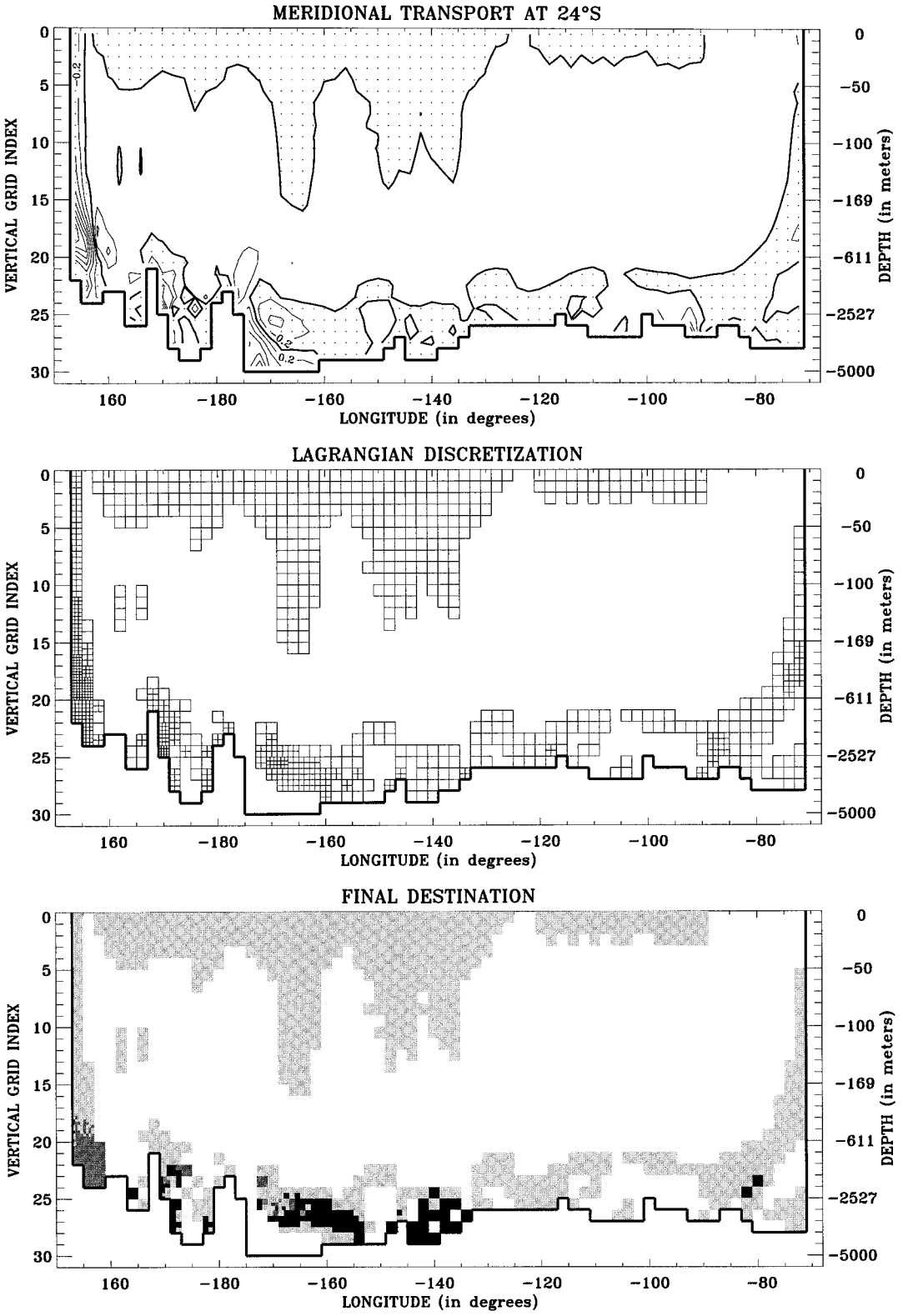

FIG. A1. Study of the southward flow from 24°S in the Pacific. (a) Annual-mean model mass flow (in Sv) with a 0.2 Sv contour interval. Dotted areas locate regions where the mean velocity is southward. (b) Initial particles distribution obtained with a maximum individual transport equal to 10^{-1} Sv (one subregion ≡ one particle). The exact distribution retained for the full analysis has a much higher accuracy and uses particles that are also lagged in time. (c) Final destination colored, as calculated, for each particle: America 65°W (black), Tasmania 145°E (dark gray), or recirculation toward Pacific 24°S (light gray).

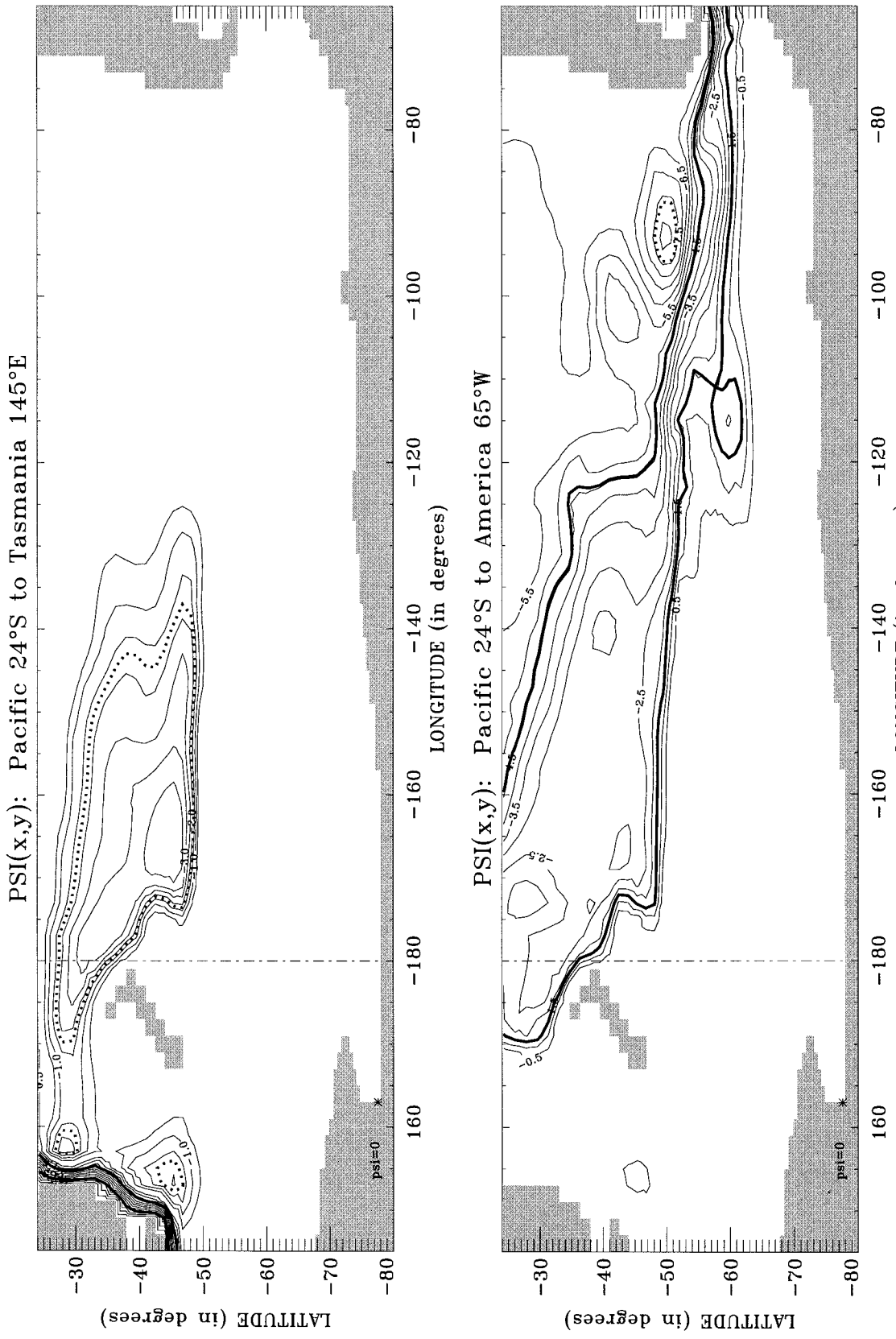

FIG. A2. Horizontal streamfunction related to the vertically integrated transport of the southward flow of Pacific 24°S water to (a) Tasmania 145°E and (b) America 65°W. The value of the streamfunctions is set to zero in Antarctica and the contour interval is 0.5 Sv. Additional bold contours isolate the pathway followed by the median half of each mass transfer and appear in Fig. 1. Thick dotted contours emphasize possible basinwide recirculations associated with these interbasin mass transports and also appear in Fig. 1.

particles, leading to a true discrimination of all water masses.

Acknowledgments. We thank Michel Arhan, Michèle Fieux, and Robert Molcard for useful discussions. It is a pleasure to acknowledge comments and suggestions by Alexandre Ganachaud and an anonymous reviewer, which greatly improved the readability of the paper. Support for this study has been provided by the Centre National de la Recherche Scientifique (CNRS) for BB and GM, the Université de Bretagne Occidentale for SS, and the Stockholms Universitet for KD. This work is also supported by grants from the European Community (TRACMASS project, Contract MAS3-CT97/0142) and by an Action Thématique Innovante from the Institut National des Sciences de l'Univers. Lagrangian calculations were performed with the computational resources available at LPO, at the Centre de Brest of the Institut Français de Recherche pour l'Exploitation de la Mer and at the Institut du Développement et des Ressources en Informatique Scientifique (CNRS).

APPENDIX

Lagrangian Analysis

Though all the ingredients of our Lagrangian analysis have already been published, it is worth summing up in this appendix its main steps, going through one example (in this case, the southward connections achieved from 24°S in the Pacific). The OGCM provides monthly maps of the cross velocity over the section in study; to simplify the representation, Fig. A1a represents only the annual-mean gridded transport flow, that is, the mean model meridional velocity multiplied by the area of each model grid cell. Next, the southward transport is described by a large number of particles, each one associated with a fraction of the flow at 24°S. As detailed in Blanke and Raynaud (1997), particles are grouped in regions where the transport is the highest: the area of each model grid cell is divided into small subregions (one subregion ≡ one particle) so as not to assign more than a prescribed maximum transport, T_0, to each particle. The distribution displayed by Fig. A1b was obtained with $T_0 = 10^{-1}$ Sv, but the exact distribution retained for the full analysis has a much higher accuracy, and uses particles that are also lagged in time, to account for the seasonality of the flow. Then, the trajectories of all particles are integrated forward in time until they reach given final sections, in this case Tasmania 145°E, America 65°W, or Pacific 24°S (for recirculating particles). The interbasin mass exchanges (or intrabasin recirculations) are calculated by summing the infinitesimal transports of the particles that achieve the same connection, as illustrated in Fig. A1c by coloring the initial section according to the fate of the particles that describe it. These exchanges amount to 7.0 Sv, 6.1 Sv, and 38.6 Sv, respectively.

Finally, we display the general movement associated with each transfer by recording the passage of each particle and summing algebraically its transport on each velocity point of the three-dimensional grid (Blanke et al. 1999). The subsequent three-dimensional nondivergent transport field is then integrated along the vertical direction. One obtains a two-dimensional nondivergent transport field that may be pictured as a streamfunction whose contours depict the general features of the connection in study. Figures A2a and A2b display the streamfunctions calculated for the mass transfers from Pacific 24°S to Tasmania 145°E and America 65°W, respectively, with a 0.5 Sv contour interval, taking a zero reference value over Antarctica. Two bold contours are added on each figure, isolating the pathway followed by the median half of each mass transfer. These contours are those used on Fig. 1 to derive the global circulation scheme.

REFERENCES

Arakawa, A., 1972: Design of the UCLA general circulation model. Numerical simulation of weather and climate. Tech. Rep. 7, Dept. of Meteorology, University of California, Los Angeles, 116 pp.

Beckmann, A., and R. Döscher, 1997: A method for improved representation of dense water spreading over topography in geopotential-coordinate models. *J. Phys. Oceanogr.,* **27,** 581–591.

Blanke, B., and P. Delecluse, 1993: Variability of the tropical Atlantic Ocean simulated by a general circulation model with two different mixed-layer physics. *J. Phys. Oceanogr.,* **23,** 1363–1388.

——, and S. Raynaud, 1997: Kinematics of the Pacific Equatorial Undercurrent: A Eulerian and Lagrangian approach from GCM results. *J. Phys. Oceanogr.,* **27,** 1038–1053.

——, M. Arhan, G. Madec, and S. Roche, 1999: Warm water paths in the equatorial Atlantic as diagnosed with a general circulation model. *J. Phys. Oceanogr.,* **29,** 2753–2768.

Döös, K., 1995: Interocean exchange of water masses. *J. Geophys. Res.,* **100,** 13 499–13 514.

Gordon, A. L., 1986: Interocean exchange of thermocline water. *J. Geophys. Res.,* **91,** 5037–5046.

——, 1995: When is appearance reality? A comment on ''Why does the Indonesian Throughflow appear to originate from the North Pacific.'' *J. Phys. Oceanogr.,* **25,** 1560–1567.

——, R. F. Weiss, W. M. Smethie Jr., and M. J. Warner, 1992: Thermocline and intermediate water communication between the South Atlantic and Indian Oceans. *J. Geophys. Res.,* **97,** 7223–7240.

——, R. D. Susanto, and A. Ffield, 1999: Throughflow within Makassar Strait. *Geophys. Res. Lett.,* **26,** 3325–3328.

Levitus, S., 1982: *Climatological Atlas of the World Ocean.* NOAA Prof. Paper No. 13, U.S. Govt. Printing Office, 173 pp. and 17 microfiche.

Lukas, R., T. Yamagata, and J. P. McCreary, 1996: Pacific low-latitude western boundary currents and the Indonesian throughflow. *J. Geophys. Res.,* **101,** 12 209–12 216.

Macdonald, A. M., and C. Wunsch, 1996: An estimate of global ocean circulation and heat fluxes. *Nature,* **382,** 436–439.

Madec, G., and M. Imbard, 1996: A global ocean mesh to overcome the North Pole singularity. *Climate Dyn.,* **12,** 381–388.

——, P. Delecluse, M. Imbard, and C. Lévy, 1998: OPA 8.1 Ocean General Circulation Model reference manual. Notes du Pôle de Modélisation de l'Institut Pierre-Simon Laplace 11, 91 pp.

Paillet, J., M. Arhan, and M. S. McCartney, 1998: Spreading of Labrador Sea Water in the eastern North Atlantic. *J. Geophys. Res.,* **103,** 10 223–10 239.

Reid, J. L., 1997: On the total geostrophic circulation of the Pacific

Ocean: Flow patterns, tracers and transports. *Progress in Oceanography,* Vol. 39, Pergamon, 263–352.

Rintoul, S. R., 1991: South Atlantic interbasin exchange. *J. Geophys. Res.,* **96,** 2675–2692.

Schmitz, W. J., Jr., 1996: Some global features/North Atlantic circulation. Vol. I. On the World Ocean circulation. Woods Hole Oceanographic Institution Tech. Rep. WHOI-96-03, 150 pp.

——, and M. S. McCartney, 1993: On the North Atlantic circulation. *Rev. Geophys.,* **31,** 29–49.

Shriver, J. F., and H. E. Hurlburt, 1997: The contribution of the global thermohaline circulation to the Pacific to Indian Ocean throughflow via Indonesia. *J. Geophys. Res.,* **102,** 5491–5511.

Sloyan, B. M., and S. R. Rintoul, 2000: Estimates of area-averaged diapycnal fluxes from basin-scale budgets. *J. Phys. Oceanogr.,* **30,** 2320–2341.

Smith, W. H. F., and D. T. Sandwell, 1997: Global sea floor topography from satellite altimetry and ship depth sounding. *Science,* **277,** 1956–1962.

Speich, S., B. Blanke, and G. Madec, 2001: Warm and cold water routes of a GCM thermohaline conveyor belt. *Geophys. Res. Lett.,* **28,** 311–314.

Tsimplis, M. N., S. Bacon, and H. L. Bryden, 1998: The circulation of the subtropical South Pacific derived from hydrographic data. *J. Geophys. Res.,* **103,** 21 443–21 468.

Whitworth, T., III, W. D. Nowlin Jr., and S. J. Worley, 1982: Net transport of the Antarctic Circumpolar Current through Drake Passage. *J. Phys. Oceanogr.,* **12,** 960–971.